



# Characterization and ammonolysis behavior of poly(isosorbide carbonate)-based copolymers

Kazuaki Rikiyama<sup>1</sup> · Akari Matsunami<sup>1</sup> · Takayuki Yoshida<sup>2</sup> · Tatsuo Taniguchi<sup>1</sup> · Takashi Karatsu<sup>1</sup> · Shotaro Nishitsuji<sup>2</sup> · Daisuke Aoki<sup>1</sup>

Received: 2 October 2023 / Revised: 5 December 2023 / Accepted: 8 December 2023 / Published online: 12 January 2024  
© The Society of Polymer Science, Japan 2024

## Abstract

The development of recyclable polymers has attracted considerable attention for realizing the development of a sustainable society. Polycarbonates (PCs) are engineering plastics with high thermal stability and transparency. We focused on poly(isosorbide carbonate) (PIC), a bio-based PC synthesized from isosorbide (ISB) derived from glucose. PIC is expected to function as an alternative to conventional PCs because of its outstanding transparency and thermal and physical properties. This study prepared PIC copolymers with several types of diol comonomers to clarify the effect of copolymerization on the decomposition reaction with ammonia, i.e., ammonolysis for converting PIC copolymers into monomers and urea. The thermal and physical properties of the resulting copolymers were also investigated. The thermal stability of the PIC copolymers remained stable after copolymerization, and the glass transition temperature was affected mainly by the flexibility of the structure of the introduced comonomer. A drastic change in mechanical properties was observed for the copolymer synthesized with 1,4-butanediol, which provides guidelines for toughening PIC with a small comonomer ratio. Finally, we investigated the decomposition behavior of the copolymers by treatment with aqueous ammonia. The PIC copolymers were decomposed into ISB, comonomers, and urea, and the ammonolysis rate was affected by the introduced structure. This study promotes the effective use of ISB as a biomass resource through ammonolysis, which is an effective chemical recycling process for polycarbonate.

## Introduction

With the increasing awareness of environmental perils, substantial efforts have been devoted to building a sustainable society. A focal point in this endeavor is the

innovative use of biomass in creating polymeric materials. This has attracted considerable attention in addressing the challenge of resource depletion linked to traditional polymers. For bio-based polymeric materials, polylactic acid [1, 2], bio-poly(ethylene terephthalate) (bioPET) [3, 4], and bio-polyethylene (bioPE) [5, 6] are the primary choices for use in consumer products. The limited use of other bio-based materials can be attributed to their high costs or subpar properties compared with those of traditional petroleum-based polymers.

Poly(isosorbide carbonate) (PIC) has attracted significant interest as a bio-based polycarbonate (PC); it is synthesized from a glucose-derived monomer, isosorbide (ISB) [7–12]. Although PIC is a bio-based polymer, it exhibits outstanding thermal and physical properties, as well as transparency; therefore, it is expected to function as an alternative to conventional PCs. Recently, we established a concept in which PICs and PIC copolymerized with mannitol (PIC-M) were used as sources of fertilizer after treatment with ammonia. PICs and PIC-M can be degraded by ammonolysis to afford a mixture of mainly ISB and urea,

**Supplementary information** The online version contains supplementary material available at <https://doi.org/10.1038/s41428-023-00878-2>.

✉ Shotaro Nishitsuji  
nishitsuji@yz.yamagata-u.ac.jp

✉ Daisuke Aoki  
daoki@chiba-u.jp

<sup>1</sup> Department of Applied Chemistry and Biotechnology, Graduate School of Engineering, Chiba University, 1-33 Yayoi-cho, Inage-ku, Chiba-shi, Chiba 263-8522, Japan

<sup>2</sup> Department of Organic Materials Science, Graduate School of Organic Materials Science, Yamagata University, Yonezawa, Yamagata992-8510Japan

which can be directly used as a fertilizer [13, 14]. Therefore, PIC-based polymers are used as promising engineering plastics and fertilizers, leading to innovative chemical recycling systems that provide solutions to the global food-production problem due to the ever-increasing human population. The advantage of the decomposition reaction is that ISB can be practically recovered quantitatively. ISB is a bio-based monomer, and its unit cost is considerably high [15–18]; thus, it would be attractive if it could be reused through chemical recycling. Many polymers made of ISB have been reported, and some are commercially available as alternatives to petroleum-derived PCs that are easily photodegraded [19–24]. It is difficult to obtain PIC with the desired physical properties; therefore, PIC is generally prepared by copolymerization [25–27]. Although the changes in physical properties due to copolymerization have been widely investigated, considerably less work has been conducted on chemical degradation due to copolymerization. Clarifying the effect of copolymerization on the decomposition reaction with ammonia, i.e., ammonolysis, which could be employed to convert PIC copolymers into monomers and urea, will provide useful information to promote the effective use of ISB as a biomass resource. This study focused on the effect of the structure introduced by copolymerization on the ammonolysis behavior of PIC copolymers. The ammonolysis of the PIC homopolymer heterogeneously occurs during the initial reaction step of decomposition in aqueous ammonia due to the hydrophobicity of PIC; however, the reaction mixture ultimately becomes homogeneous because ISB and urea are water-soluble compounds. Therefore, the hydrophobicity of the introduced comonomer could affect the reactivity during ammonolysis. In this study, the thermal and mechanical properties of the PIC copolymers were also investigated. The point of this study is that copolymers functionalized with small amounts of comonomers with ISB highlight the effect of the chemical structure of the comonomers on the ammonolysis behavior, which are randomly incorporated into the polymer main chain during polycondensation. Although differences in the bulkiness and reactivity of hydroxy groups on comonomers can affect monomer sequences, i.e., whether the sequences are random or block-like, when the feed ratio of a comonomer is high, a randomly incorporated comonomer in the polymer main chain can be easily obtained when the feed ratio of the comonomer in the melt polycondensation process is small. Here, 1,4-butanediol, 1,6-hexanediol, 1,4-cyclohexanediol, and 1,4-cyclohexanedimethanol were selected as comonomers because they have been used as comonomers in scientific reports and patents [28–30]. The alkyl length, structure, and ratio of these comonomers were expected to affect the rigidity of the PIC chain and/or the

interaction between the polymer chains, which is crucial for various properties, including the ammonolysis behavior. We investigated the decomposition process of the copolymers to obtain a mixture of ISB and comonomers with aqueous ammonia by nuclear magnetic resonance (NMR) spectroscopy and gel permeation chromatography (GPC). The decomposed monomers, especially ISB, are expected to be reused for repolymerization and other chemical processes.

## Materials

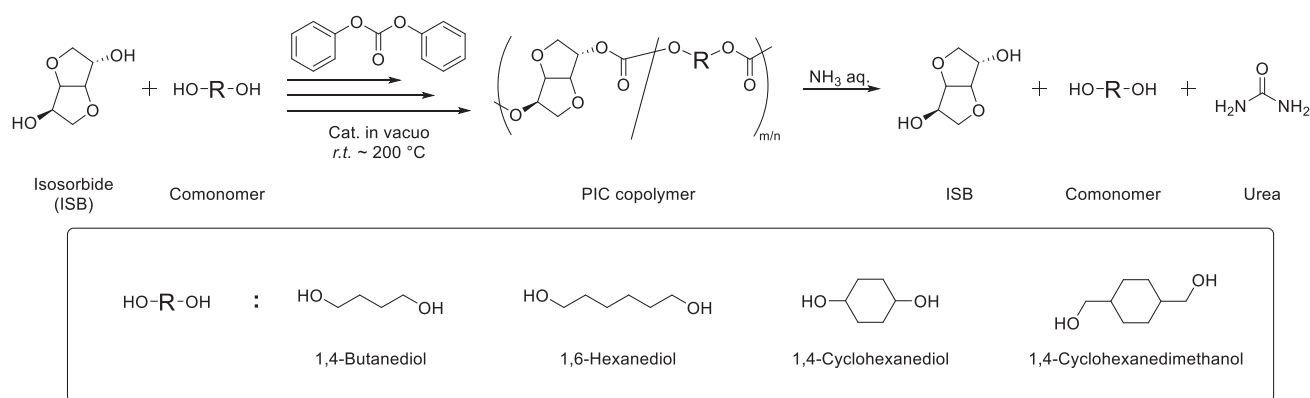
All reagents and solvents were purchased from Tokyo Chemical Industry (Tokyo, Japan), Kanto Chemical (Tokyo, Japan), FUJIFILM Wako Pure Chemical Corporation (Tokyo, Japan), and Sigma–Aldrich (MO, USA) and were used as received.

## Measurement

$^1\text{H}$  NMR magnetic resonance (NMR) spectra were recorded on a Bruker AVANCE III HD 400 M and AVANCE NEO 500 spectrometer in dimethyl sulfoxide- $d_6$  (DMSO- $d_6$ ) or chloroform- $d$  ( $\text{CDCl}_3$ ) at 25 °C. For diffusion-ordered NMR spectroscopy (DOSY), the LED method was used (pulse program: ledbpgp2s; diffusion time: 100 ms; diffusion gradient length: 2000  $\mu\text{s}$ ; maximum gradient strength: 51 G/cm in DMSO- $d_6$  at 25 °C) [31]. Gel permeation chromatography (GPC) was performed at 40 °C on a JASCO HSS-1500 system with a guard column (TOSOH TSKgel® guardcolumn SuperH-L), three columns (TOSOH TSKgel® SuperH 6000, 4000, and 2500), and a refractive index (RI) detector. *N,N*-Dimethylformamide (DMF) with lithium bromide (5 mM) was used as the eluent for GPC at a flow rate of 0.6 ml min $^{-1}$ . Polystyrene standards (number average molecular weight ( $M_n$ ) 1920–2630,000 g mol $^{-1}$ ; polydispersity index (PDI) = 1.03–1.08) were used to calibrate the GPC system. The thermal decomposition temperature ( $T_{d-5\%}$ ) values of the synthesized polymers were estimated by thermogravimetric analysis (TGA) on a SHIMADZU DTG-60A system, and all samples were heated to 550 °C at a rate of 10 °C min $^{-1}$  under an ambient atmosphere. The glass transition temperature ( $T_g$ ) values of the synthesized PIC copolymers were estimated using differential scanning calorimetry (DSC) on a SHIMADZU DSC-60A Plus instrument at a heating rate of 10 °C min $^{-1}$  under a flow of  $\text{N}_2$ .

## Synthesis of PIC copolymers

PIC copolymers were synthesized via a one-pot polycondensation method in which the transesterification and



**Scheme 1** Synthesis and ammonolysis of PIC copolymers

polycondensation reactions were conducted in the same reactor continuously. For all comonomers, the syntheses were performed by the same procedure described below. ISB, diphenyl carbonate (DPC), comonomer and lithium acetylacetonate (LiAcac) were placed in a two-necked round-bottomed flask (200 mL) equipped with a mechanical stirrer. In the transesterification stage, the reactants were heated to 180 °C under a N<sub>2</sub> atmosphere and stirred for 2 h. After that, the temperature was increased to 200 °C and maintained for 30 min. During the polycondensation stage, the reaction system was continuously stirred under vacuum (ca. 10 mmHg) at 200 °C for 30 min and then under high vacuum (<1 mmHg) at 200 °C for 1.5 h to remove phenol. After the reaction was finished, the reaction system was cooled to room temperature while remaining in a N<sub>2</sub> atmosphere. The product was dissolved in chloroform, followed by precipitation from methanol. After filtration and drying under vacuum, the PIC copolymer was obtained as a white solid. The ratio of comonomers in the feed was set to 10% and 20% to vary their mole fraction in the copolymers.

### Mechanical analysis

Sample films were obtained by heat pressing. Sample powders were dried in a vacuum oven at 80 °C for 12 h before being subjected to molding by a heat press. Heat pressing was performed using an MP-SC heating press machine (Toyo Seiki Seisaku-Sho, Ltd.). The press temperature was 240 °C for PIC and 220 °C for the other samples. Each sample was 150 μm thick, 20 mm wide, and 40 mm long. These films were punched into dumbbell specimens with a stripe portion 2 mm in width and 12 mm in length (JIS-6251-7) and tested via uniaxial tensile testing. Uniaxial tensile testing was carried out at 25 °C using an EMX-1000N-FA tensile tester (IMADA CO.,LTD). The crosshead speed was 5 mm min<sup>-1</sup>. The stress and strain

were calculated by using the initial cross-sectional area and the initial length.

### Ammonolysis of PIC copolymers

PIC and PIC copolymers containing 10% comonomer (ca. 300 mg) were placed into a 50 mL reactor. Ammonia solution was added to the reactor at 20 times the amount of carbonate bonds in the polymer. The reaction mixture was heated and stirred at 30, 60, or 90 °C in an oil bath for 48 h. After 12, 24, and 48 h, a portion of the reaction mixture was placed in a vial, followed by freeze-drying to remove the ammonia and water. The products were dissolved in DMF and/or DMSO-*d*<sub>6</sub> for use in GPC and <sup>1</sup>H NMR spectroscopy analyses to evaluate the ammonolysis behavior of the PIC copolymers.

## Results and discussion

### Synthesis of PIC copolymers

As shown in Scheme 1, ISB and each comonomer were combined with diphenyl carbonate (DPC) as the carbonyl source and LiAcac as the catalyst. The copolymerization was conducted as a one-pot melt polycondensation reaction in which transesterification and polycondensation occurred consecutively in the same reactor. The ratio of ISB to comonomers in the PIC copolymers was controlled by varying the feed ratio in the reaction system. Poly(isosorbide carbonate-*co*-butyl carbonate) (**P(IC-*co*-BC)**), poly(isosorbide carbonate-*co*-hexyl carbonate) (**P(IC-*co*-HC)**), poly(isosorbide carbonate-*co*-cyclohexyl carbonate) (**P(IC-*co*-CHC)**), and poly(isosorbide carbonate-*co*-dime-thylcyclohexyl carbonate) (**P(IC-*co*-CMC)**) were obtained by copolymerization with 1,4-butanediol, 1,6-hexanediol, 1,4-cyclohexanediol, and 1,4-cyclohexanedimethanol, respectively. The copolymers were obtained as white solids,

**Fig. 1** GPC profiles of PIC copolymers: **a** P(IC-co-BC)s, **b** P(IC-co-HC)s, **c** P(IC-co-CHC)s, and **d** P(IC-co-CMC)s

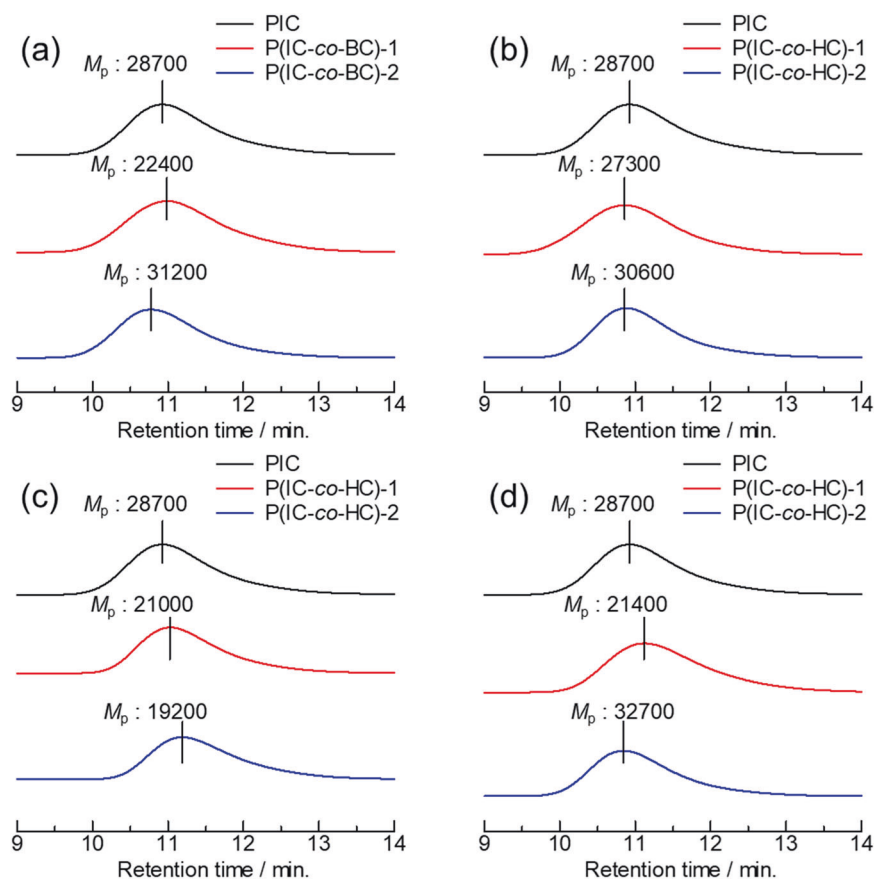


**Table 1** Molecular weight, mole fraction of comonomer, glass transition temperature ( $T_g$ ), and 5%-weight loss temperature ( $T_{d-5\%}$ ) of the PIC copolymers

Sample ID	Yield (%)	ISB:Diol <sup>a</sup>	$M_n^b$	$M_w/M_n^b$	$T_{d-5\%}^c$ (°C)	$T_g^d$ (°C)
PIC	97	–	13900	2.20	312	163
P(IC-co-BC)-1	97	0.91:0.09	10100	1.88	306	142
P(IC-co-BC)-2	82	0.81:0.19	10400	2.02	303	126
P(IC-co-HC)-1	92	0.91:0.09	11400	1.95	307	138
P(IC-co-HC)-2	96	0.81:0.19	15700	2.02	303	106
P(IC-co-CHC)-1	95	0.89:0.11	11300	1.84	293	155
P(IC-co-CHC)-2	93	0.81:0.19	9820	1.87	284	148
P(IC-co-CMC)-1	98	0.91:0.09	10400	2.17	311	139
P(IC-co-CMC)-2	97	0.81:0.19	15700	2.13	318	134

<sup>a</sup>Determined by  $^1\text{H}$  NMR (400 MHz, 25 °C,  $\text{CDCl}_3$ ) <sup>b</sup>Determined by GPC (eluent: DMF; detector: refractive index (RI); calibration: polystyrene (PS) standards) <sup>c</sup>Determined by TGA (heating rate of 10 °C  $\text{min}^{-1}$ ) <sup>d</sup>Determined by DSC; DSC data refer to the second heating at a heating rate of 10 °C  $\text{min}^{-1}$

and the number-average molecular weight determined by GPC with *N,N*-dimethylformamide (DMF) as the eluent (Fig. 1) was approximately 10,000. All the chromatograms showed unimodal distributions, and the polydispersity index (PDI) range was 1.8–2.2. The mole fractions of ISB and the comonomers in the PIC copolymers were calculated based on the integration ratios of signals in the  $^1\text{H}$ NMR spectra (Figs. S1–4). The results correlated with the feed ratio, indicating that the comonomers had been successfully introduced (Table 1).

## Thermal properties

The thermal properties of the synthesized PIC copolymers were investigated by differential scanning calorimetry (DSC) and thermogravimetric analysis (TGA) (Table 1). These results were compared with those of a PIC homopolymer with a similar molecular weight, which was synthesized using the procedure in a previous report [13]. The  $T_{d-5\%}$  values of all the PIC copolymers, except P(IC-co-CMC), slightly decreased. However, they were still high

**Fig. 2** TGA curves of PIC copolymers: **a** P(IC-co-BC)s, **b** P(IC-co-HC)s, **c** P(IC-co-CHC)s, and **d** P(IC-co-CMC)s

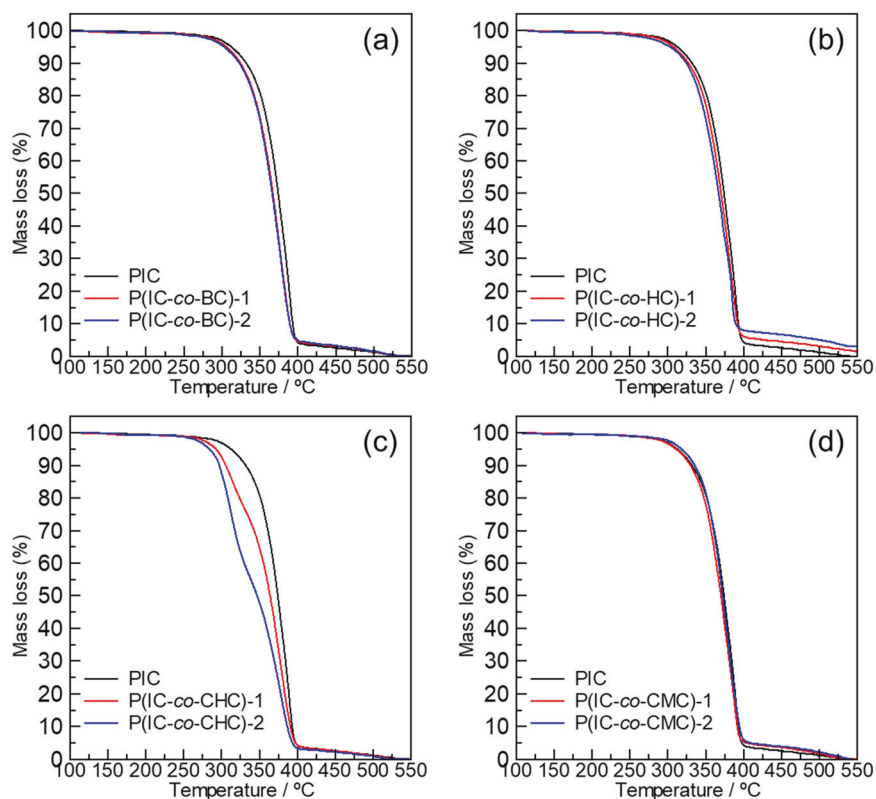
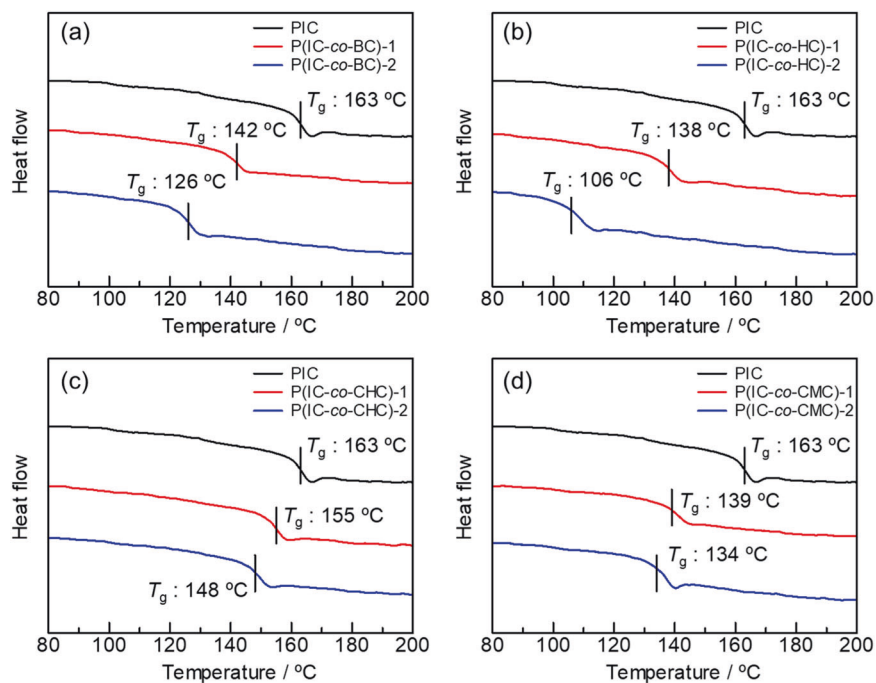


**Fig. 3** DSC profiles of PIC copolymers: **a** P(IC-co-BC)s, **b** P(IC-co-HC)s, **c** P(IC-co-CHC)s, and **d** P(IC-co-CMC)s



(>280 °C), and the thermal decomposition of the PIC and PIC copolymers proceeded within similar temperature ranges (Fig. 2). Thus, comonomers were introduced into PIC without a loss in their thermal stability. The thermal decomposition of P(IC-co-CHC) was observed to be a two-

step process. The first decrease in the TGA curves increased with increasing comonomer ratio; therefore, the first step might be due to the degradation induced by the introduced 1,4-cyclohexanediol groups. It is supposed that the  $T_{d-5\%}$  value of P(IC-co-CHC)-2 decreased with an increasing



ratio of introduced comonomer, which promoted the first weight loss of the TGA curve. The  $T_{d-5\%}$  values of **P(IC-co-CMC)** were comparable to that of the PIC homopolymer. This indicated that the introduction and ratio of 1,4-cyclohexanedimethanol did not significantly affect the  $T_{d-5\%}$  value of **P(IC-co-CMC)**, which was consistent with the findings of previous reports.

The  $T_g$  values of the PIC copolymers were lower than those of the PIC homopolymer (Fig. 3). This was caused by the mobility of the polymer chain. PIC is rigid because it is constructed using ISB, which includes two condensed heterocyclic structures. The structures introduced by the copolymerization were alkyl groups (**P(IC-co-BC)** and **P(IC-co-HC)**) and cycloalkyl groups (**P(IC-co-CHC)** and **P(IC-co-CMC)**), which are flexible compared with the ISB-derived structure. Interestingly, among the PIC copolymers with similar mole fractions of the comonomer, the  $T_g$  values may reflect the flexibility of the introduced structures. For example, the  $T_g$  value of **P(IC-co-BC)-1** exceeded that of **P(IC-co-HC)**. This was consistent with the conformational degree of freedom of alkyl groups. The  $T_g$  value of

**P(IC-co-CHC)-1** exceeded that of **P(IC-co-CMC)-1** because the methylene group adjacent to the six-membered ring contributed to the flexibility of the main chain. The  $T_g$  values of the PIC copolymers decreased with increasing comonomer ratio. In particular, the  $T_g$  value (106 °C) of **P(IC-co-HC)-2** was lower than that of PIC by more than 50 °C, although the mole fraction of the hexanediol-derived part was only 20%. The introduced hexyl group supposedly had a higher conformational degree of freedom than the other groups in the main chain. The  $T_g$  values of **P(IC-co-HC)-2** were still higher than that of polystyrene (PS), which is known as a commodity plastic [32, 33]. This result indicated that the structural factor of the comonomer was as significant as its mole fraction in the PIC copolymer. The DSC analysis results suggested that all the comonomers were randomly incorporated into the polymer main chain. The resulting copolymers were expected to highlight the effect of the chemical structure of the comonomer on the ammonolysis process.

## Mechanical properties

Figure 4 shows the stress–strain (S–S) curves of PIC and the PIC copolymers. PIC yielded and necked as the strain increased. The necking did not propagate and broke as soon as it occurred. **P(IC-co-BC)-1** broke before yielding. **P(IC-co-BC)-1** could be molded but was too brittle and could not uniaxially elongate well. Conversely, **P(IC-co-BC)-2** necked after yielding, after which the necking propagated and subsequently fractured. The yield stress, stress at break, and tensile modulus decreased compared with those of PIC; however, the strain at break drastically increased. As a result, the fracture energy was more than double that of PIC. This was achieved by adding 20% butyl groups, which resulted in ductile fracture. This drastic change in mechanical properties should be highlighted because only 20% butyl groups were introduced into PIC, which provides a guideline for toughening PIC (Table 2). For **P(IC-co-HC)**, the yield stress, stress at break, and elastic modulus decreased as the comonomer ratio increased. In contrast, the strain at break was practically unchanged for **P(IC-co-HC)-2** compared with that for PIC but increased for **P(IC-co-HC)-1**. A comparison of **P(IC-co-BC)-2** and **P(IC-co-HC)-1**, which resulted in

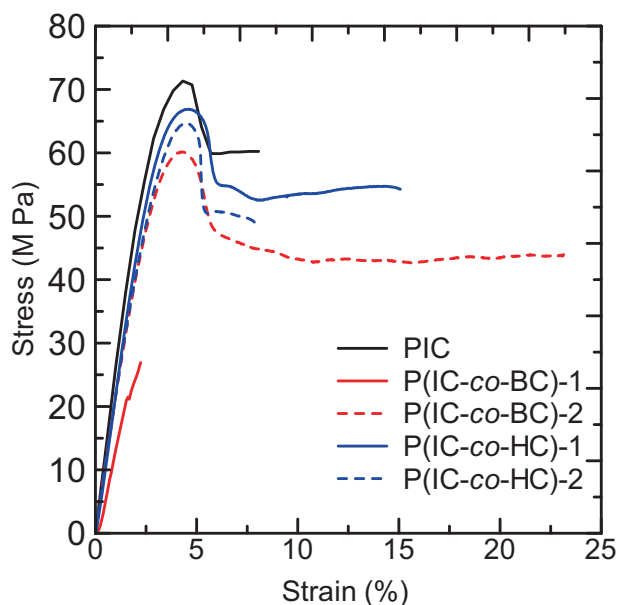


**Fig. 4** S–S curves of **PIC**, **P(IC-co-BC)-1**, **P(IC-co-BC)-2**, **P(IC-co-HC)-1**, and **P(IC-co-HC)-2**

**Table 2** Mechanical properties of the PIC copolymers

Sample ID	Yield stress (MPa)	Strain at break	Stress at break (MPa)	Tensile modulus (GPa)	Fracture energy (MJ m <sup>-3</sup> )
PIC	71.3	0.0806	60.2	2.66	4.32
P(IC-co-BC)-1	-	0.0223	26.9	1.58	0.312
P(IC-co-BC)-2	60.2	0.231	44.0	2.25	10.1
P(IC-co-HC)-1	66.9	0.151	54.3	2.33	7.76
P(IC-co-HC)-2	64.7	0.0787	49.0	2.19	3.63

ductile fracture, revealed that **P(IC-co-HC)-1** exhibited a slightly lower strain at break. However, other tensile properties, such as yield stress, stress at break, and tensile modulus, were higher. Interestingly, for the PIC copolymers containing hexyl groups, the fracture energy was comparable to that of PIC; however, the effect of the comonomer ratio was the opposite between butyl and hexyl groups. The other samples (**P(IC-co-CHC)-1**, **P(IC-co-CHC)-2**, **P(IC-co-CMC)-1**, **P(IC-co-CMC)-2**) were too brittle to be molded.

Park et al. systematically investigated the mechanical properties of a copolymer copolymerized with 1,4-cyclohexanedimethanol, referred to as **P(IC-co-CMC)** in the present study, in response to the comonomer ratio [24]. Although the mechanical properties of PIC-based copolymers with a high comonomer ratio have been extensively studied, particularly in industry, only a limited number of studies focusing on PIC-based copolymers with a low comonomer ratio, which were targeted in the present study, have been conducted. This is because the mechanical properties of PIC-based polymers are affected by molecular weight and PDI. Accordingly, catalyst research on PIC-based polymers is ongoing [7, 8, 10–12]. The mechanical properties of the polymers synthesized in the present study are described herein; however, since the influence of molecular weight is noticeable, further investigation is required to determine whether this influence is due to the chemical structure generated from copolymerization.

## Ammonolysis

To compare the ammonolysis behaviors of PIC and copolymers, PIC with a molecular weight ( $M_n$ ) of 13,900 and PDI of 2.2 was synthesized and used as a reference. The ammonolysis reaction was conducted under mild conditions that would allow insufficient decomposition to highlight the change in the degradation behavior of the copolymers during the initial ammonolysis reaction, i.e., 30 °C with 20 equivalents of ammonia relative to the carbonate linkage content in the polymers.

Ammonolysis heterogeneously occurred during the initial reaction stage owing to the poor solubility of the PIC-based copolymer in water. The reaction mixture of the PIC homopolymer gradually became homogeneous and completely transparent after 48 h. The reaction mixture of **P(IC-co-BC)** practically became transparent but remained slightly powdery and cloudy after 48 h. **P(IC-co-HC)**, **P(IC-co-CHC)**, and **P(IC-co-CMC)** were turbid during the reaction (Figure S5).

After removing water and ammonia by freeze-drying a portion of the reaction mixture, the obtained products were characterized. The ammonolysis behavior was characterized

using the residual polymer ratio ( $[M_p]_t/[M_p]_0$ ), i.e., the ratio of the peak-top molecular weight at a given reaction time ( $[M_p]_t$ ) relative to the initial value ( $[M_p]_0$ ).  $[M_p]_t/[M_p]_0 = 0$  indicated the complete absence of polymers in the degradation products; the  $[M_p]$  values were estimated using the GPC profiles during the reaction (Fig. 5a and S6–S9). The  $[M_p]_t/[M_p]_0$  values showed that after 48 h, **P(IC-co-BC)** and **P(IC-co-CHC)** were completely decomposed into small molecules; however, **P(IC-co-HC)** and **P(IC-co-CMC)** were not. In particular, the  $[M_p]_t/[M_p]_0$  value of **P(IC-co-HC)** was the highest among the copolymers, and the  $^1\text{H}$  NMR spectrum of the reaction solution of **P(IC-co-HC)** exhibited peaks derived from polymerized ISB and 1,6-hexanediol, indicating an extremely low ammonolysis rate (Figure S10). The GPC profile of **P(IC-co-CMC)** also exhibited a polymer peak (Figure S9); however, its  $[M_p]_t/[M_p]_0$  value was lower than that of **P(IC-co-HC)** after 48 h, and its  $^1\text{H}$  NMR spectrum did not exhibit peaks corresponding to polymerized ISB (Figure S12). Other small peaks that were not assigned were signals of the reaction intermediates of ammonolysis, e.g., derivatives with carbamate esters on hydroxy groups of ISB and/or comonomer [13]. Figure 6 shows that the yellow highlighted peaks (b and e) assigned to a proton in the polymerized ISB disappeared, and the peaks derived from ISB increased as the reaction proceeded, indicating that the polymerized ISB was decomposed into monomers. The  $[M_p]_t/[M_p]_0$  plots showed that the decomposition of **P(IC-co-BC)** and **P(IC-co-CHC)** was rapid compared with that of **P(IC-co-HC)** and **P(IC-co-CMC)**, indicating that the ammonolysis rate was affected by the introduced structure.

Subsequently, the ammonolysis reaction was performed under relatively severe conditions for all the samples to reveal the effect of the chemical structure of the comonomer on decomposition, i.e., at 60 °C with 20 equivalents of ammonia relative to the carbonate bond content in the polymers. The reaction mixture of the PIC homopolymer gradually became homogeneous and completely transparent after 12 h, and that of **P(IC-co-BC)** became transparent after 48 h. Conversely, **P(IC-co-HC)**, **P(IC-co-CHC)**, and **P(IC-co-CMC)** remained turbid (Figure S13). The  $[M_p]_t/[M_p]_0$  values in Fig. 5a and b indicated that the polymeric compound was almost fully degraded during ammonolysis at 60 °C, indicating that decomposition at 60 °C proceeded faster than that at 30 °C. In addition, the ammonolysis reaction rate varied depending on the introduced comonomer. In particular, the ammonolysis of **P(IC-co-CMC)** was the slowest among those of the copolymers under these conditions.

Thereafter, ammonolysis was performed under harsh conditions that would allow sufficient decomposition to proceed at 90 °C with 20 equivalents of ammonia relative to the carbonate bond content in the polymers. The reaction mixture of the PIC homopolymer became homogeneous and

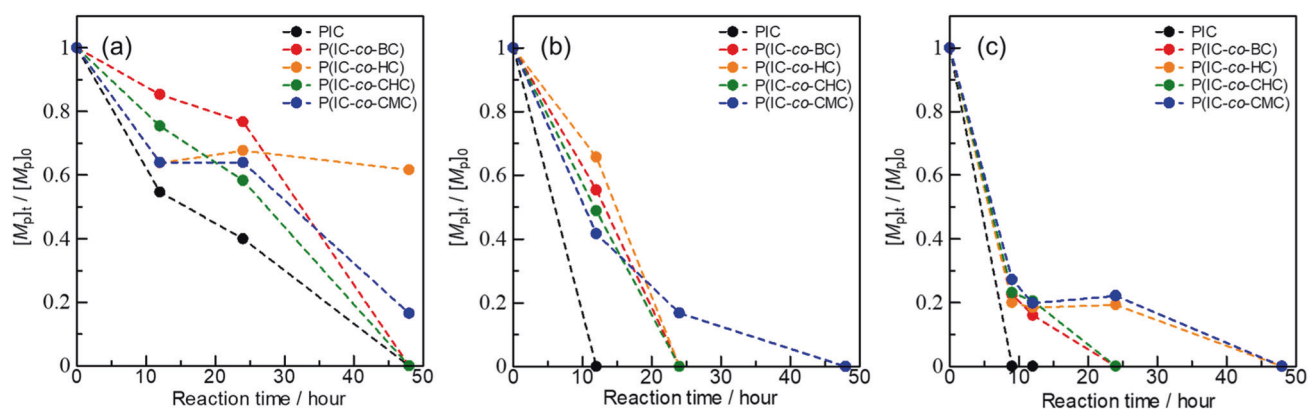
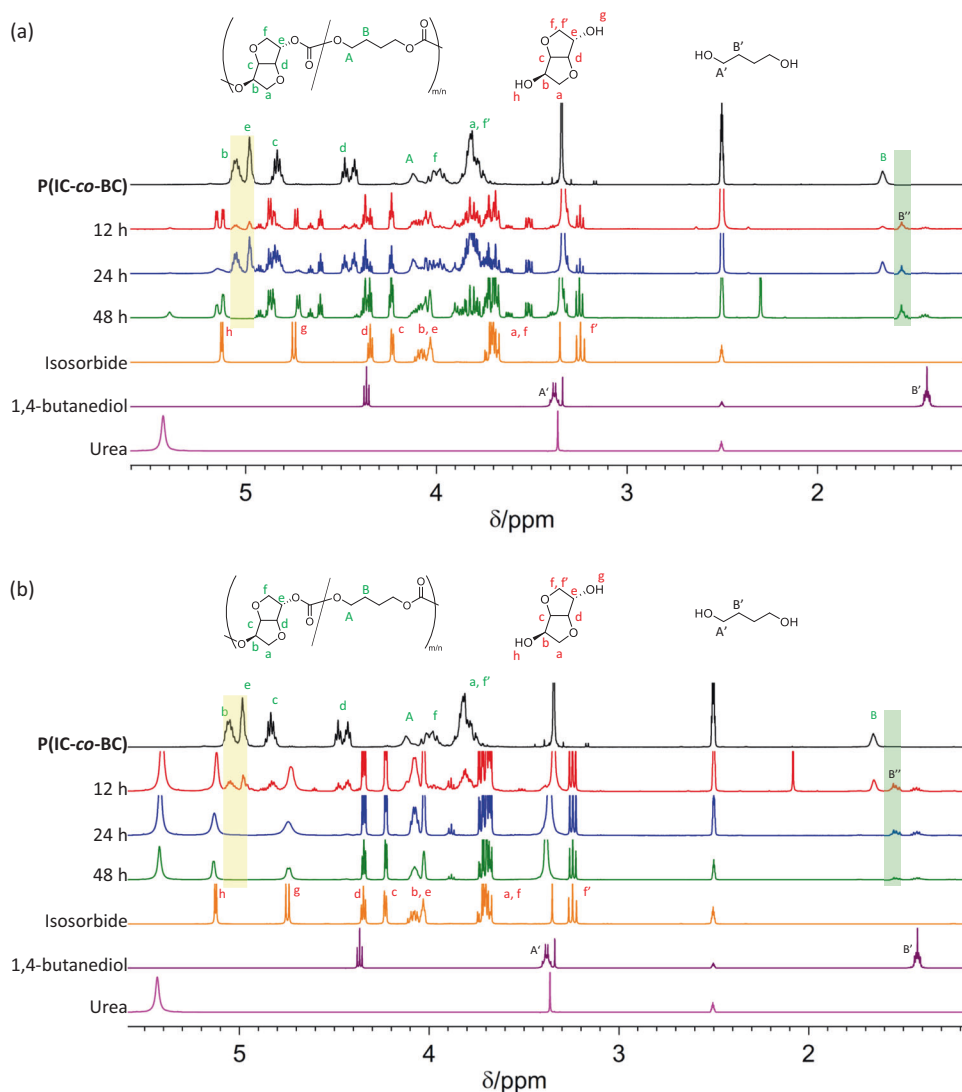


**Fig. 5** Residual polymer ratio ( $[M_{p,t}]/[M_{p,0}]$ ) values estimated using GPC profiles during ammonolysis at **a** 30 °C, **b** 60 °C, and **c** 90 °C

**Fig. 6**  $^1\text{H}$  NMR spectra of **P(IC-co-BC)** before (black) and after the reaction at 12 h (red), 24 h (blue), and 48 h (green) at **a** 30 °C and **b** 90 °C. The yellow highlighted peak was derived from the polymerized ISB part; it disappeared in proportion to the reaction time, indicating decomposition. The green highlighted peak was derived from the reaction intermediate



transparent after 6 h. The reaction solution of the PIC copolymers was also transparent. However, upon careful observation, the samples appeared to aggregate and adhere to the stirrer chip as viscous solids (Fig. 5c and S23).

Although the GPC profile indicated that the polymeric compound disappeared, there were small amounts of solid in the reaction mixture after 48 h (Fig. 7 and S23–25). These solids were assumed to be a reaction intermediate, i.e., a



**Fig. 7** GPC profiles of the reaction solution of **P(IC-co-BC)** during ammonolysis at 90 °C with 20 equivalents of ammonia relative to carbonate bonds. The left side is an enlarged view, and the right side is an overall view

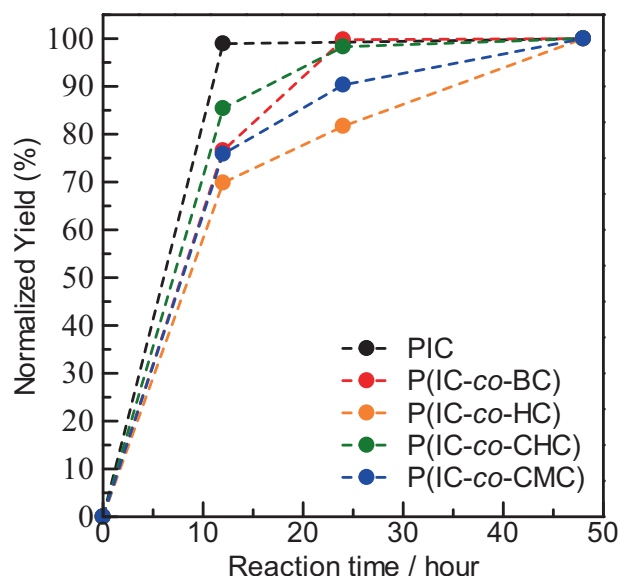
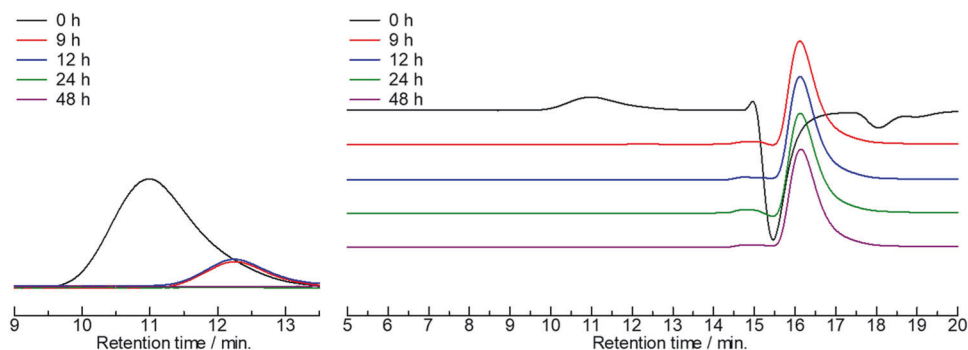


**Fig. 8** Normalized ISB yield estimated from the  $^1\text{H}$  NMR spectra

carbamate ester of 1,4-butanediol. As shown in Fig. 6, two peaks at approximately 1.45 (B') and 1.55 (B'') ppm appeared and grew in proportion to the reaction time. The ratio of the integrated signal from ISB to these peaks (1.2–1.8 ppm) correlated with the copolymer ratio; therefore, these new peaks were assigned to reaction intermediates mainly comprising comonomers. The peak at approximately 1.45 ppm was assigned to the methylene groups of 1,4-butanediol (Fig. 6). The results of diffusion-ordered spectroscopy (DOSY) revealed that the new peaks at approximately 1.55 ppm represented a diffusion coefficient smaller than those of the comonomer peaks (Figure S29). Furthermore, to confirm the existence of the reaction intermediate, we synthesized 1,4-butanediol dicarbamate (**BuD-DC**), which could be produced by the partial decomposition of the carbonate bonds combined with 1,4-butanediol with ammonia (see Figures S30–S31). Figure S31 shows that the  $^1\text{H}$  NMR spectral peak at approximately 1.55 ppm could be assigned to the methylene groups of **BuD-DC**. Interestingly, although the PIC copolymers were decomposed under the harsh conditions (90 °C), a slight amount of **BuD-DC** remained in the

reaction mixture, indicating that the decomposition rate of the reaction intermediates was very slow. Similar results were obtained in the case of other PIC copolymers, indicating that the carbamates of the introduced comonomer were not fully degraded during the reaction. These results indicated that the polymerized ISB parts were preferentially decomposed before the comonomer part during ammonolysis of the PIC copolymers (Figures S26–28). Previously, we introduced the mannitol unit as a hydrophilic comonomer, and ammonolysis preferentially occurred around the mannitol unit. Interestingly, in the present study, the introduction of a hydrophobic unit resulted in the opposite behavior [14].

Finally, the normalized yield of ISB was estimated from the  $^1\text{H}$  NMR spectra as a percentage of the integrated signal of ISB (c) relative to that of the entire spectrum (Fig. 8). The decomposition of the ISB parts in the PIC copolymers was observed to be slower than that in the PIC homopolymer. In particular, the degradation of the ISB parts in **P(IC-co-HC)** was the slowest among the polymers. These results showed that the introduced hydrophobic comonomer dominated the ammonolytic reactivity by changing the solubility of the PIC copolymers and decomposition intermediate, as well as by causing aggregation in an aqueous medium.

We confirmed that the decomposition rate was dependent on the type of comonomer in the polymer main chain. The structure introduced by copolymerization affected the ammonolysis reaction rate and the behavior in aqueous media; therefore, proper conditions are required for the decomposition of PIC copolymers. Although the type of comonomer is important for thermal and mechanical properties, as well as the decomposition rate in aqueous media, even at a small copolymerization ratio, it is more important that PIC-based copolymers can be decomposed and afford ISB and urea without side reactions if enough ammonia and a high enough temperature are employed for decomposition.

## Conclusions

Here, **PIC**, which is expected to function as an alternative to conventional oil-based PCs, was functionalized by

copolymerization at a small ratio. Its thermal and physical properties were characterized, and its degradability during ammonolysis was determined. All the PIC copolymers were successfully synthesized with a known ratio of ISB to comonomer, which was simply accomplished by adding the comonomer to the reaction system. Thermal analysis of the PIC copolymers revealed that the ratio of the comonomer and the structural factor of the comonomer significantly affected the thermal and mechanical properties of the copolymers. The flexibility of the PIC copolymers due to the conformational degree of freedom of the introduced structure was reflected in the decrease in  $T_g$ . These results suggested that the proper choice of comonomer, even at a small copolymerization ratio, could enable the design of PIC-based copolymers with extremely extensive properties, such as **P(IC-co-BC)-2**. During ammonolysis, the degradation speed was affected by the type of comonomer and its ratio in the polymer main chain. Importantly, the PIC-based copolymers were completely decomposed and afforded monomers and urea without side reactions. We expect that the study findings will promote the effective use of ISB as a biomass resource through the use of ammonolysis as an effective chemical recycling process.

**Acknowledgements** This work was supported by the JST CREST grant JPMJCR22L1.

## Compliance with ethical standards

**Conflict of interest** The authors declare no competing interests.

## References

- Inkinen S, Hakkarainen M, Albertsson A-C, Södergård A. From Lactic Acid to Poly(lactic acid) (PLA): Characterization and analysis of PLA and its precursors. *Biomacromolecules*. 2011; 12:523–32.
- Chen G-Q, Patel MK. Plastics derived from biological sources: present and future: a technical and environmental review. *Chem Rev*. 2012;112:2082–99.
- Pang J, Zheng M, Sun R, Wang A, Wang X, Zhang T. Synthesis of ethylene glycol and terephthalic acid from biomass for producing PET. *Green Chem*. 2016;18:342–59.
- Cui Y, Deng C, Fan L, Qiu Y, Zhao L. Progress in the biosynthesis of bio-based PET and PEF polyester monomers. *Green Chem*. 2023;25:5836–57.
- Siracusa V, Blanco I. Bio-Polyethylene (Bio-PE), Bio-Polypropylene (Bio-PP) and Bio-Poly(ethylene terephthalate) (Bio-PET): Recent developments in bio-based polymers analogous to petroleum-derived ones for packaging and engineering applications. *Polymers*. 2020;12:1641.
- Hayes G, Laurel M, MacKinnon D, Zhao T, Houck H, Becer CR. Polymers without petrochemicals: sustainable routes to conventional monomers. *Chem Rev*. 2023;123:2609–734.
- Eo YS, Rhee H-W, Shin S. Catalyst screening for the melt polymerization of isosorbide-based polycarbonate. *J Ind Eng Chem*. 2016;37:42–46.
- Zhang M, Lai W, Su L, Lin Y, Wu G. A synthetic strategy toward isosorbide polycarbonate with a high molecular weight: The effect of intermolecular hydrogen bonding between isosorbide and metal chlorides. *Polym Chem*. 2019;10:3380–9.
- Ochoa-Gómez JR, Gil-Río S, Maestro-Madurga B, Gómez-Jiménez-Aberasturi O, Río-Pérez F. Synthesis of isosorbide bis(methyl carbonate) by transesterification of isosorbide with dimethyl carbonate, and evidence of its usefulness as a monomer for manufacturing polycarbonates. *Arab J Chem*. 2019;12:4764–74.
- Qian W, Ma X, Liu L, Deng L, Su Q, Bai R, et al. Efficient synthesis of bio-derived polycarbonates from dimethyl carbonate and isosorbide: Regulating: exo-OH and endo-OH reactivity by ionic liquids. *Green Chem*. 2020;22:5357–68.
- Zhang Z, Xu F, He H, Ding W, Fang W, Sun W, et al. Synthesis of high-molecular weight isosorbide-based polycarbonates through efficient activation of endo-hydroxyl groups by an ionic liquid. *Green Chem*. 2019;21:3891–901.
- Qian W, Liu L, Zhang Z, Su Q, Zhao W, Cheng W, et al. Synthesis of bioderived polycarbonates with adjustable molecular weights catalyzed by phenolic-derived ionic liquids. *Green Chem*. 2020;22:2488–97.
- Abe T, Takashima R, Kamiya T, Foong CP, Numata K, Aoki D, et al. Plastics to fertilizers: chemical recycling of a bio-based polycarbonate as a fertilizer source. *Green Chem*. 2021;23:9030–7.
- Abe T, Kamiya T, Otsuka H, Aoki D. Plastics to fertilizer: guiding principles for functionable and fertilizable fully bio-based polycarbonates. *Polym Chem*. 2023;14:2469–77.
- Hockett RC, Fletcher HG, Sheffield EL, Goepf RM Jr. Hexitol Anhydrides.<sup>1</sup> The Structure of Isosorbide, a Crystalline Dianhydrosorbitol.<sup>2</sup> *J Am Chem Soc*. 1946;68:927–30.
- Hoffer BW, Crezee E, Devred F, Mooijman PRM, Sloof WG, Kooyman PJ, Van Langeveld AD, Kapteijn F, Moulijn JA. The role of the active phase of Raney-type Ni catalysts in the selective hydrogenation of D-glucose to D-sorbitol. *Appl Catal, A*. 2003;253:437–52.
- Schimpf S, Louis C, Claus P. Ni/SiO<sub>2</sub> catalysts prepared with ethylenediamine nickel precursors: Influence of the pretreatment on the catalytic properties in glucose hydrogenation. *Appl Catal, A*. 2007;318:45–53.
- Dussenne C, Delaunay T, Wiatz V, Wyart H, Suisse I, Sauthier M. Synthesis of isosorbide: An overview of challenging reactions. *Green Chem*. 2017;19:5332–44.
- Guerrero AR, Ramírez JC. Photodegradation of poly(methyl methacrylate)/ bisphenol A polycarbonate blends. *Polym Bull*. 1994;33:541–8.
- Li Q, Zhu W, Li C, Guan G, Zhang D, Ziao Y, et al. A non-phosgene process to homopolycarbonate and copolycarbonates of isosorbide using dimethyl carbonate: Synthesis, characterization, and properties. *J Polym Sci, A: Polym Chem*. 2013;51:1387–97.
- Lee CH, Takagi H, Okamoto H, Kato M. Preparation and mechanical properties of a copolycarbonate composed of bio-based isosorbide and bisphenol A. *Polym J*. 2015;47:639–43.
- Yokoe M, Aoi K, Okada M. Biodegradable polymers based on renewable resources. VII. Novel random and alternating copolycarbonates from 1,4:3,6-dianhydrohexitols and aliphatic diols. *J Polym Sci, A: Polym Chem*. 2003;41:2312–21.
- Han R, Kida T, Yamaguchi M. Viscoelastic properties of copolycarbonates comprising isosorbide and 1,4-cyclohexanedimethanol. *Colloid Polym Sci*. 2023;301:1231–8.
- Park S-A, Choi J, Ju S, Jegal J, Lee KM, Hwang SY, et al. Copolycarbonates of bio-based rigid isosorbide and flexible 1,4-cyclohexanedimethanol: Merits over bisphenol-A based polycarbonates. *Polymer*. 2017;116:153–9.
- Kricheldorf HR, Sun S-J, Gerken A, Chang T-C. Polymers of Cholesteric polycarbonates derived from (S)-((2-Methylbutyl)thio)hydroquinone or Isosorbide. *Macromolecules*. 1996;29:8077–82.

26. Ma C, Xu F, Cheng W, Tan Z, Su Q, Zhang S. Tailoring molecular weight of bioderived polycarbonates via bifunctional ionic liquids catalysts under metal-free conditions. *ACS Sustain Chem Eng*. 2018;6:2684–93.
27. Hult D, García-Gallego S, Ingverud T, Andrén OCJ, Malkoch M. Degradable high  $T_g$  sugar-derived polycarbonates from isosorbide and dihydroxyacetone. *Polym Chem*. 2018;9:2238–46.
28. Chatti S, Kricheldorf HR, Schwarz G. Copolycarbonates of isosorbide and various diols. *J Polym Sci, A: Polym Chem*. 2006;44:3616–28.
29. Fang W, Zhang Z, Yang Z, Zhang Y, Xu F, Li C, et al. One-pot synthesis of bio-based polycarbonates from dimethyl carbonate and isosorbide under metal-free condition. *Green Chem*. 2020; 22:4550–60.
30. Yang Z, Zhang Z, Fu M, Wang W, Shi Y, Li C, et al. One-pot synthesis of isosorbide-based copolycarbonate with good flexibility and tunable thermal property. *J Macromol Sci Part A: Pure Appl Chem*. 2021;58:398–407.
31. Yu D, Zhong J, Pu Z, Hou H, Li X, Zhu R, et al. Synthesis and properties of biobased polycarbonate based on isosorbitol. *J Polym Res*. 2023;30:204.
32. Wu DH, Chen AD, Johnson CS. An Improved Diffusion-Ordered Spectroscopy Experiment Incorporating Bipolar-Gradient Pulses. *J Magn Reson Ser A*. 1995;115:260–4.
33. Rieger J. The glass transition temperature of polystyrene. *J Therm Anal*. 1996;46:965–72.

**Publisher's note** Springer Nature remains neutral with regard to jurisdictional claims in published maps and institutional affiliations.

Springer Nature or its licensor (e.g. a society or other partner) holds exclusive rights to this article under a publishing agreement with the author(s) or other rightsholder(s); author self-archiving of the accepted manuscript version of this article is solely governed by the terms of such publishing agreement and applicable law.